# Simplified Model of Machado-Joseph Disease in Comparison to Parkinson's Disease and Normal Models

**Anjulie Agrusa**
M.S. Student of Bioengineering
UC San Diego
San Diego CA

**Mike Aquino**
M.Eng. Student of Bioengineering
UC San Diego
San Diego CA

**Julia Hardy**
Ph.D. Student of Bioengineering
UC San Diego
San Diego CA

**M. Fikret Yalcinbas**
M.Eng. Student of Bioengineering
UC San Diego
San Diego CA

## Abstract

A Hodgkin-Huxley model was constructed in MATLAB with seven neurons that collectively represent each of the main regions of the brain. One model affected by Parkinson's Disease (PD) and a Machado-Joseph Disease (MJD) model were developed using the orignal healthy model as a basis. To simplify the model given the limited resources regarding MJD activity, all conductance values and equilibrium potentials are standard across all regions of the brain. The bulk current and behaviors between the regions are represented through synaptic or inhibitory connections. Therefore, adjusting the synaptic strengths and/or inhibitory power between the neurons within the healthy model such that the brain mimics PD and MJD, created the two unique disease models. In order to accurately compare the behaviors of the networks, we used uniformly scaled current across the disease models. Given an external current to the Substantia Nigra at the beginning of the network, we observed the spiking frequencies of the cortex, represented as the final neuron in the network. The cortex neuron is presumed to excite the motor cortex, thus causing the motor deficit symptoms. Our hypothesis was that we can infer whether the network resembles a PD or MJD by observing the output spiking behavior in response to known currents.

## 1 Background and significance

Misdiagnosis of Parkinson's (PD) and Machado-Joseph disease (MJD) is a result of their similar initial symptoms. The symptoms of Parkinson's (tremors, rigidity, slowness of movement, and impaired balance and coordination) overlaps with the symptoms of Machado-Joseph Disease (progressive clumsiness, staggering lurching gait, difficulty with speech and swallowing, and impaired eye movement). However, the diseases affect the brain differently.

Parkinson's is a motor system disorder caused by a loss of dopamine-producing brain cells. It affects the Substantia Nigra, Striatum, Globus Pallidus Externa, Globus Pallidus Internal, and Thalamus regions of the brain [1]. The disease usually affects people over 60, but early onset Parkinson's can occur as young as 21.

Machado-Joseph disease is a movement disorder caused by a polyglutamine-encoding CAG

repeat mutation of ATXN3 gene [2]. It affects the Striatum and Subthalamic Nucleus regions of the brain primarily, but other studies have shown other areas of affect as well [3]. Typical onset is as early as 10 and as late as 70 years of age with the average maximum life expectancy at 30 years from onset. The disease eventually leads to a complete loss of function of muscles and organs.

The goal of our project is to construct models of the brain affected by both PD and MJD that can exhibit discernible behaviors when given the neural parameters associated with the respective pathologies of the diseases, all of which is based from the diagram (Figure 1). By creating an objective, measurable algorithm that takes the neural input and output of the affected regions into consideration, we hope to reliably predict which disease is being presented in the patient

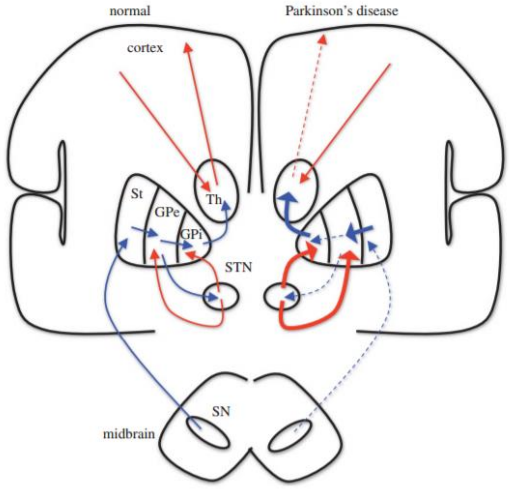


Figure 1 – Model of healthy brain connectivity versus unhealthy brain connectivity. (Adapted from [1])

# 2 Methods

The seven-neuron network is constructed based on Figure 1. Each neuron in the network is modeled by the Hodgkin Huxley model[1] (Eq. 1). The voltage differential equations for each neuron, as well as each gating variable (Eq. 2-5) are solved for as a system of 35 ordinary differential equations via MATLAB's ODE23. The channel opening and closing rate functions ($\alpha$ and $\beta$) are shown in equations 6-15. They are evaluated as functions of each neuron's specific membrane voltage. Because the whole neural network is modeled as a system of ordinary differential equations, these channel's opening and closing rate functions can be dynamically evaluated for a fluctuating membrane voltage.

## 2.1 Models

The healthy control neural network (Fig. 2) is modified in order to replicate the pathology present in PD. The synaptic currents flowing from the Substantia Nigra, Globus Pallidus Externa, and Thalamus are scaled down by a factor of two. Computationally, this is done by reducing the inhibitory synaptic current on the Striatum, Subthalamic Nucleus, and Globus Pallidus Internal, and reducing the excitatory synaptic current on the Cortex. Additionally, the synaptic currents flowing from the Subthalamic Nucleus are scaled up by a factor of two. Computationally this is done by increasing the excitatory synaptic current on the Striatum and Globus Pallidus Internal. The complete PD neural network model can be seen in Figure 3.

[1] All parameters such as conductance values, equilibrium potentials, etc. are found in the Appendix.

The healthy control neural network (Fig. 2) is modified in order to replicate the pathology present in MJD. The synaptic currents flowing from the Striatum and Subthalamic Nucleus are scaled down by a factor of three. Computationally, this is done by reducing the inhibitory synaptic current acting on the Globus Pallidus Externa, and reducing the excitatory synaptic current on the Striatum and Globus Pallidus Internal. The complete Machado Joseph's neural network model can be seen in Figure 4.

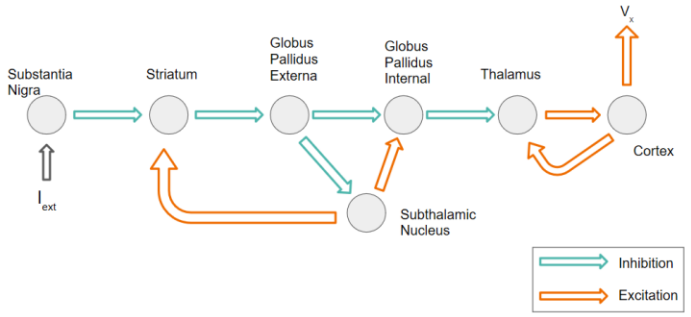


Figure 2 - Healthy control neural network

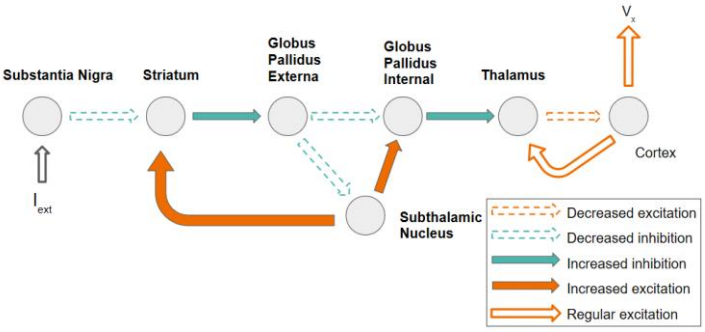


Figure 3 - Parkinson's Disease neural network

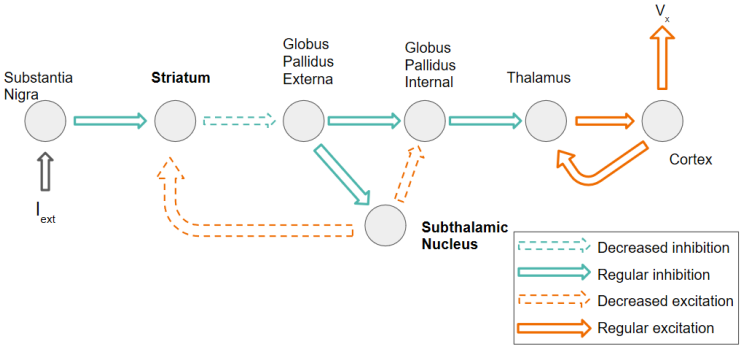


Figure 4 - Machado-Joseph Disease neural network

All three neural network models are evaluated from 0 to 500 milliseconds, with an external current of 6.5[2] μA/cm$^2$. A fast Fourier transform is computed in MATLAB. The number of samples is found by computing the length of any of the voltage vectors. The sampling rate is calculated by dividing the number of samples by 0.5 seconds. The magnitude of the fast Fourier transform (FFT) is plotted against the relevant frequency range.

### 2.2 Data collection

A spike counter is implemented in all three models by recording the number of local maxima with voltages greater than 80 mV within 50 ms. Additionally, the mean interspike interval for each model is computed[3]. The spike threshold was set to 30 mV, as to discount any subthreshold activity. A random number generator selects 500 external current values between 6.5 and 70μA/cm2. All three neural network models are evaluated for the same 500 external current values. The respective mean interspike intervals and number of spikes are used as feature vectors. The number of spikes feature is modified slightly to take into account the external current. The external current being tested is divided by the number of spikes value, thus giving the dynamic number of spikes feature used for classification. Of the 500 trials for each model, 70% of the feature-label pairs are used for training a logistic regression classifier [4]. Training and testing data is split using Scikit-Learn's Train-Test-Split function. The remaining 30% of the feature pairs are classified via a binary classifier. The normal vs. Parkinson's model is tested, the normal vs. MJD model is tested, and the Parkinson's vs. MJD model is tested. The Train_Test_Split function splices the feature data randomly, yielding slight variations in classification results each time. Thus, each binary classifier is run five times and averaged.

### 2.3 Equations

$$\frac{dV}{dt} = \frac{1}{C}\left(-I_{Na} - I_K - I_L + I_{ext}\right) \quad \text{Eq. 1}$$

$$\frac{dm}{dt} = \alpha_m(V)\,(1-m) - \beta_m(V)\,m \quad \text{Eq. 2}$$

$$\frac{dh}{dt} = \alpha_h(V)\,(1-h) - \beta_h(V)\,h \quad \text{Eq. 3}$$

$$\frac{dn}{dt} = \alpha_n(V)\,(1-n) - \beta_n(V)\,n \quad \text{Eq. 4}$$

$$\frac{dr}{dt} = \alpha_r[T]\,(1-r) - \beta_r\,r \quad \text{Eq. 5}$$

$$\alpha_m(V) = (25-V)/(10*(\exp((25-V)/10)-1)) \quad \text{Eq. 6}$$

$$\beta_m(V) = 4\,\exp(-V/18) \quad \text{Eq. 7}$$

$$\alpha_h(V) = 0.07\,\exp(-V/20) \quad \text{Eq. 8}$$

$$\beta_h(V) = 1/(\exp((30-V)/10)+1) \quad \text{Eq. 9}$$

[2] This external current was experimentally determined to be the smallest current for which the Substantia Nigra shows continual firing.

[3] The mean interspike interval is computed via MATLAB function isi.m, created by BENG 260 teaching department.

Eq. 10 $$\alpha_n(V) = (10 - V)/(100 * (\exp((10 - V)/10) - 1))$$

Eq. 11 $$\beta_n(V) = 0.125 \exp(-V/80)$$

Eq. 12 $\alpha_{r\_Inhibitory}=5$

Eq. 13 $\beta_{r\_Inhibitory}= 0.18$

Eq. 14 $\alpha_{r\_Excitatory}=2.4$

Eq. 15 $\beta_{r\_Inhibitory}= 0.56$

Eq. 16 FeatureNew=IextFeature

# 3 Results

In order to understand the difference between the normal model, the Parkinson's model, and the Machado-Joseph model, we analyzed the spiking frequency of the cortex neuron at external currents of 6.5 µA and 16.5 µA.

## 3.1 External current input at 6.5 µA

Serving as a control, the excitation of the Cortex neuron is first modeled under normal conditions, as seen in Figure 4. By comparing the normal model to the Parkinson's model, it is evident there is an increase in spike count and frequency (Figure 5). However, when the normal model is compared to the Machado-Joseph model (Figure 6), there is a decrease in spike count and a similar frequency.

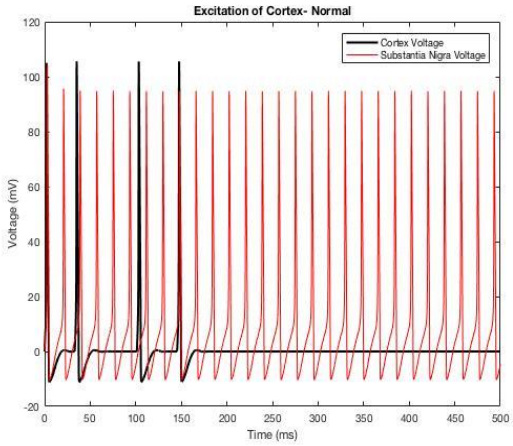


Figure 5 - The spiking patterns associated with the excitation of the Substantia Nigra neuron and the Motor Cortex neuron at an external current of 6.5 µA in the normal model.

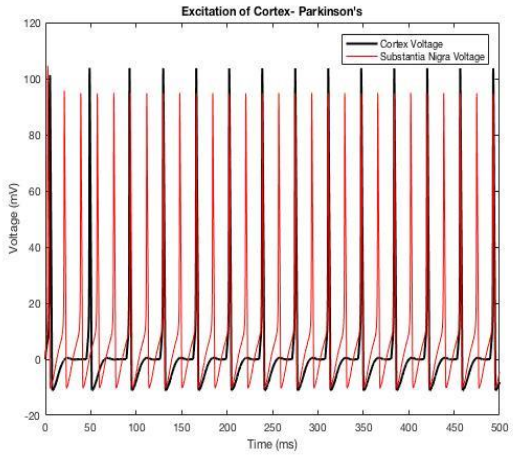


Figure 6 - The spiking patterns associated with the excitation of the Substantia Nigra neuron and the Motor Cortex neuron at an external current of 6.5 μA in the Parkinson's model.

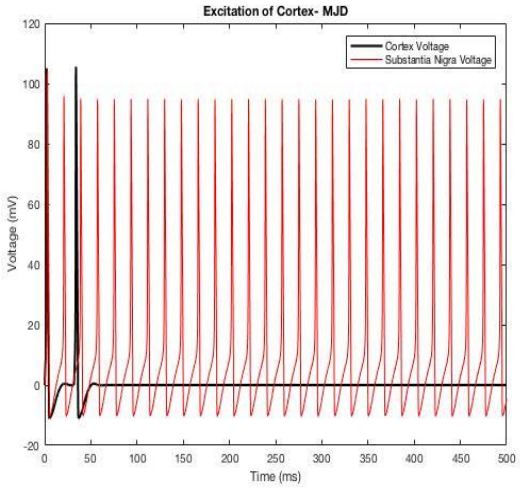


Figure 7 - The spiking patterns associated with the excitation of the Substantia Nigra neuron and the Motor Cortex neuron at an external current of 6.5 μA in the Machado-Joseph model.

Figures 8-10 show the FFT of the normal, Parkinson's and Machado-Joseph models. By looking at the frequency peaks, the normal model and the Machado-Joseph model have nearly identical peak locations, while the Parkinson's model has peaks in different locations.

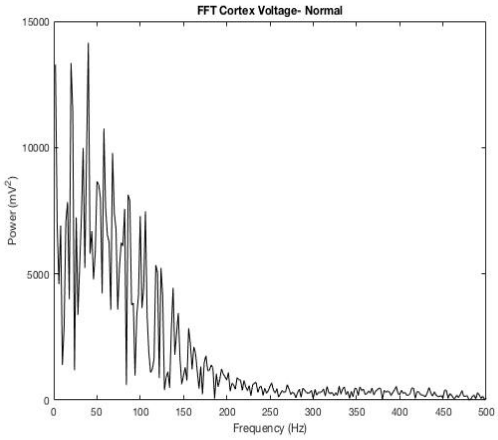


Figure 8 - Fast Fourier Transform of the normal model at 6.5 µA.

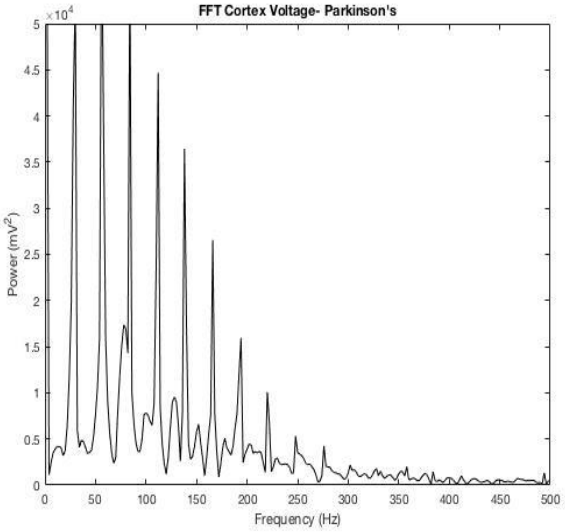


Figure 9 - Fast Fourier Transform of the Parkinson's model at 6.5 µA.

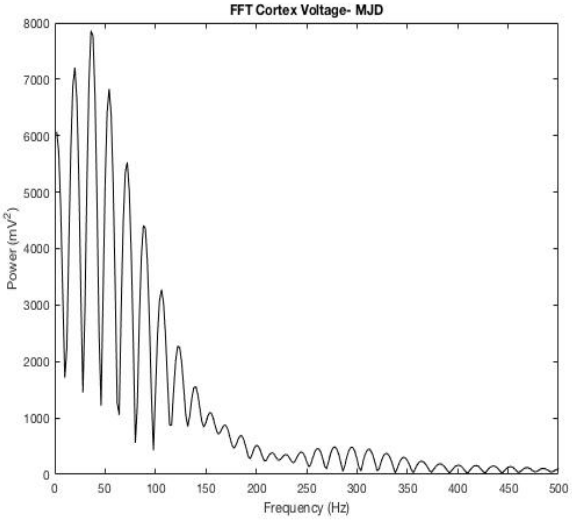


Figure 10 - Fast Fourier Transform of the Machado-Joseph model at 6.5 µA.

### 3.2 External current input at 16.5 µA

Now the same analysis is done at an external current of 16.5 µA, as seen in Figures 11-13. The normal and Machado-Joseph models are now nearly identical. The Parkinson's model still has increased spike count.

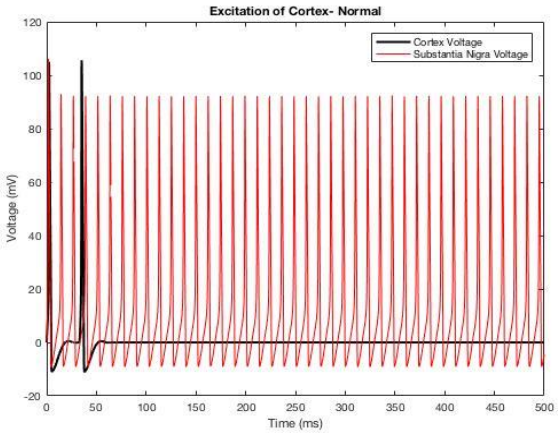


Figure 11 - The spiking patterns associated with the excitation of the Substantia Nigra neuron and the Motor Cortex neuron at an external current of 16.5 µA in the normal model.

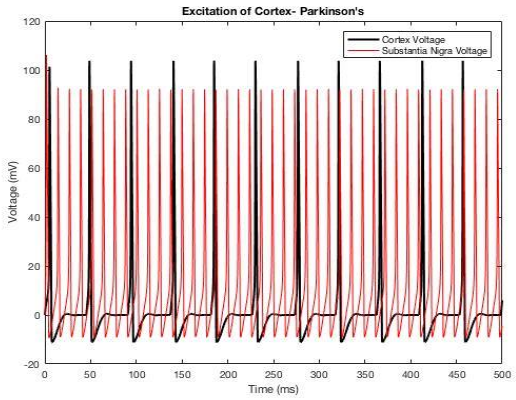


Figure 12 - The spiking patterns associated with the excitation of the Substantia Nigra neuron and the Motor Cortex neuron at an external current of 16.5 µA in the Parkinson's model.

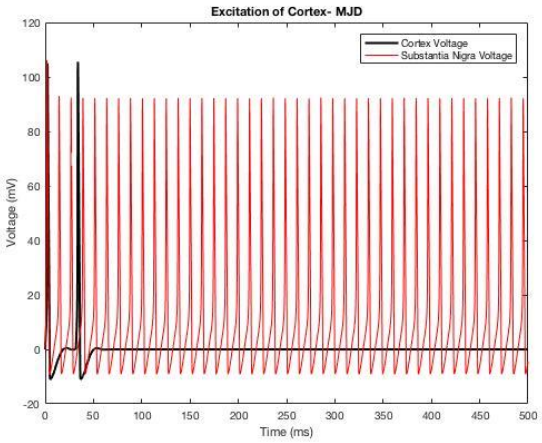


Figure 13 - The spiking patterns associated with the excitation of the Substantia Nigra neuron and the Motor Cortex neuron at an external current of 16.5 µA in the Machado-Joseph model.

The FFT of the three models at 16.5 µA result in Figures 14-16. Unlike at 6.5 µA, the Frequency spikes are now all at nearly identical locations. This makes it much more difficult to discern between the three different cases.

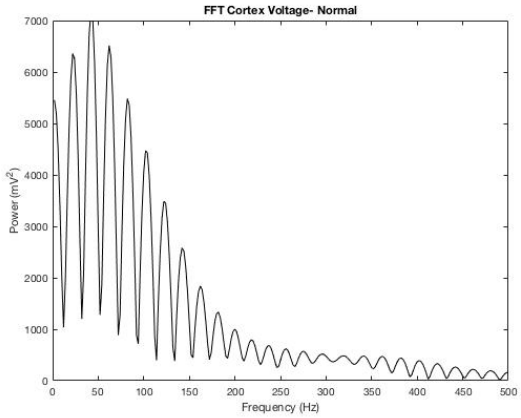


Figure 14 - Fast Fourier Transform of the normal model at 16.5 µA.

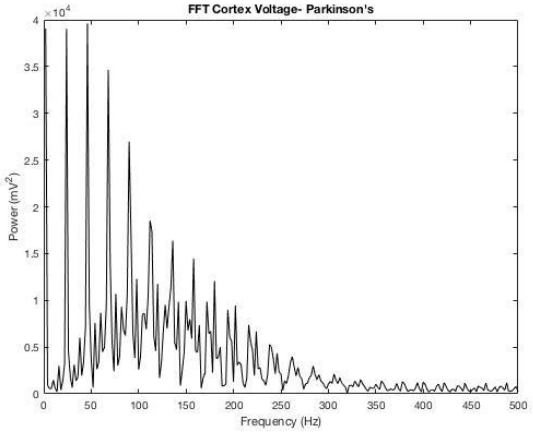


Figure 15 - Fast Fourier Transform of the Parkinson's model at 16.5 µA.

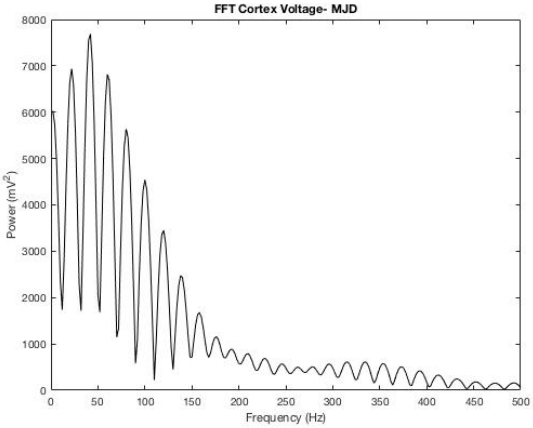


Figure 16 - Fast Fourier Transform of the Machado-Joseph model at 16.5 µA.

### 3.3 Statistical analysis on number of spikes and interspike interval

#### 3.3.1 Current weighted features

Figure 17 shows the current-weighted feature space. Spatially, a class separation can be seen with regard to PD vs. healthy and PD vs. MJD.

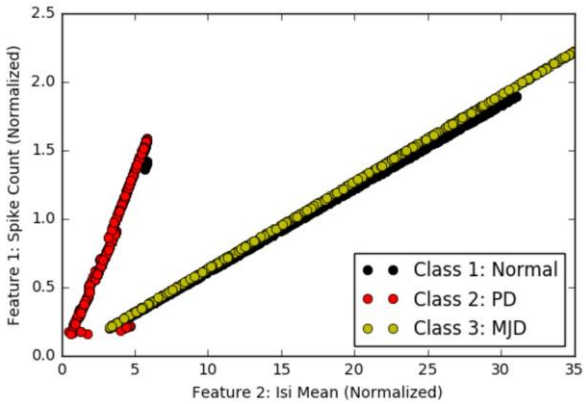


Figure 17 - Feature 1 vs. Feature 2 for Current- Weighted Features

As seen from the table below, the model is able to classify normal vs. PD and PD vs. MJD with very high accuracy (Table 1). The model could not accurately classify the normal vs. MJD spiking patterns. Therefore, this paradigm cannot be used as a diagnostic tool for MJD. However, if a patient was displaying symptoms that could be indicative of PD or MJD, then knowledge of the current flowing into the Substantia Nigra and spiking features at the cortex could yield a diagnosis with up to 99.13% accuracy.

Table 1

| Models Tested | Classification Accuracy (%) | | | | | |
|---|---|---|---|---|---|---|
| | Trial 1 | Trial 2 | Trial 3 | Trial 4 | Trial 5 | Average |
| Healthy vs. Parkinson's | 94.33 | 91.33 | 93.67 | 92.67 | 94.00 | 93.20 |
| Healthy vs. MJD | 53.67 | 57.00 | 59.33 | 56.33 | 56.00 | 56.47 |
| Parkinson's vs. MJD | 99.67 | 99.00 | 99.00 | 99.67 | 98.33 | 99.13 |

#### 3.3.2 Current-blind features

Figure 18 shows the current-blind feature space. Spatially, a class separation can be seen between all three models. In Fig. 18 it appears that the normal and MJD features have little to no variance. One reason for this could be that the interspike intervals for the normal and MJD models are of a different scale than the interspike intervals of the Parkinson's model.

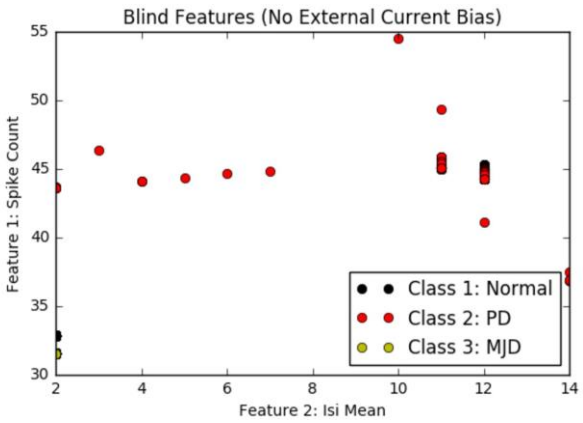


Figure 18 – Spike count versus isi mean.

As seen from the table below, the model is again able to classify normal vs. Parkinson's and Parkinson's vs. MJD with very high accuracy (Table 2). Similar to the current-weighted simulation, the model could not accurately classify the normal vs. MJD spiking patterns. This classification method had no knowledge of the external current coming into the Substantia Nigra. The classification accuracy is slightly less than when the features were recorded in relation to the external current (Section 3.3.1). However, the accuracy was still very high. Now if the patient's cortex spiking features alone are measured, a diagnosis between Parkinson's and MJD can be made with 98.67% accuracy.

Table 2

| Models Tested | Classification Accuracy (%) | | | | | |
|---|---|---|---|---|---|---|
| | Trial 1 | Trial 2 | Trial 3 | Trial 4 | Trial 5 | Average |
| Healthy vs. Parkinsons | 91.67 | 89.00 | 92.33 | 91.00 | 91.33 | 91.07 |
| Healthy vs. MJD | 53.67 | 59.33 | 58.33 | 58.67 | 58.33 | 57.67 |
| Parkinsons vs. MJD | 98.67 | 97.33 | 99.33 | 99.00 | 99.00 | 98.67 |

# 4 Conclusions and future considerations

Due to the similarity in symptoms, Machado Joeseph's disease and Parkinson's disease are often misdiagnosed in the early stages. Although both ailments affect similar areas of the brain, the changes that occur on the electrical connections cause the victims to behave differently in later stages. However, by the time the patient has reached these late stages, the patient may have been given an improper diagnosis. The goal of the experiments was to verify that PD and MJD can be properly diagnosed and differentiated from each other using the electrical output generated at the cortex. With a range of 97.33 to 99.66 percent accuracy in both blind and weighted features, PD and MJD can be distinguished from each other. The models are inconclusive when comparing MJD or PD to a healthy brain, however, the problem of differentiation, in this simple case only, has been addressed.

The results suggest that the algorithm may be capable of differentiating PD from MJD in clinical cases. This would require an accurate measurement of potential at the substantia nigra

and the cortex. Due to the limitations in current electrode technology, this model may not be suited. However, more complex models can be built for more accuracy in results or to analyze the reactions of individual neurons could be beneficial for diagnostic purposes.

## Acknowledgments

All sections of the paper were equally distributed among all four members.

## References

[1] Schiff, S. J. (2011). Towards model-based control of Parkinson's disease: A perspective. IEEE Conference on Decision and Control and European Control Conference. doi:10.1109/cdc.2011.6160870.

[2] Schmidt, T., Landwehrmeyer, G. B., Schmitt, I., Trottier, Y., Auburger, G., Laccone, F., . . . Riess, O. (1998). An Isoform of Ataxin-3 Accumulates in the Nucleus of Neuronal Cells in Affected Brain Regions of SCA3 Patients. Brain Pathology, 8(4), 669-679. doi:10.1111/j.1750-3639.1998.tb00193.x

[3] Alves, S., Regulier, E., Nascimento-Ferreira, I., Hassig, R., Dufour, N., Koeppen, A., . . . Almeida, L. P. (2008). Striatal and nigral pathology in a lentiviral rat model of Machado-Joseph disease. Human Molecular Genetics, 17(14), 2071-2083. doi:10.1093/hmg/ddn106

[4] Coleman, T. (2015, November). Logistic Regression. Lecture presented at UC San Diego, San Diego.

## Appendix

| Parameter | Value |
|---|---|
| Membrane Capacitance ($C_m$) | 1 μF/cm$^2$ |
| Conductance of Potassium ($g_K$) | 36 mS/cm$^2$ |
| Conductance of Sodium ($g_{Na}$) | 120 mS/cm$^2$ |
| Conductance of Leaky Current ($g_L$) | 0.3 mS/cm$^2$ |
| Conductance of GABA ($g_{GABA}$) | 0.5 mS/cm$^2$ |
| Conductance of Glutamate ($g_{GLU}$) | 0.2 mS/cm$^2$ |
| Equilibrium Potential of Potassium ($E_K$) | -12 mV |
| Equilibrium Potential of Sodium ($E_{Na}$) | 115 mV |
| Equilibrium Potential of Chloride ($E_{Cl}$) | -70 mV |
| Equilibrium Potential of Leaky Current ($E_L$) | 10.613 |
| T Equation | T=TMax1+ e(-(VPre-VP)/KP)) |
| $T_{Max}$ | 1.5 mM |
| $V_P$ | 77 mV |
| $K_P$ | 5 mV |